



ORIGINAL ARTICLE

Quantitative magnetic resonance neurographic characterization of peripheral nerve involvement in manifest and pre-ataxic spinocerebellar ataxia type 3

Jennifer Kollmer¹  | Markus Weiler²  | Georges Sam² | Jennifer Faber^{3,4} | John M. Hayes⁵ | Sabine Heiland^{1,6} | Martin Bendszus¹ | Wolfgang Wick^{2,7} | Heike Jacobi²

¹Department of Neuroradiology, Heidelberg University Hospital, Heidelberg, Germany

²Department of Neurology, Heidelberg University Hospital, Heidelberg, Germany

³Department of Neurology, Bonn University Hospital, Bonn, Germany

⁴German Center for Neurodegenerative Diseases, Bonn, Germany

⁵Department of Neurology, University of Michigan, Ann Arbor, USA

⁶Division of Experimental Radiology, Department of Neuroradiology, Heidelberg University Hospital, Heidelberg, Germany

⁷Clinical Cooperation Unit Neurooncology, German Cancer Research Center/DKTK, Heidelberg, Germany

Correspondence

Jennifer Kollmer, Department of Neuroradiology, Heidelberg University Hospital, Im Neuenheimer Feld 400, Heidelberg D-69120, Germany.
Email: jennifer.kollmer@med.uni-heidelberg.de

Heike Jacobi, Department of Neurology, Heidelberg University Hospital, Im Neuenheimer Feld 400, Heidelberg D-69120, Germany.
Email: heike.jacobi@med.uni-heidelberg.de

Funding information

The study was supported in part by the Medical Faculty of the University of Heidelberg (Olympia Morata stipend grant to J.K. and H.J.) and the German Research Foundation (SFB 1118 to S.H., SFB 1158 to M.B.)

Abstract

Background and purpose: Knowledge about the exact underlying pathophysiological changes involved in the genesis and progression of spinocerebellar ataxia type 3 (SCA3) is limited. Lower extremity peripheral nerve lesions in clinically, genetically and electrophysiologically classified ataxic and pre-ataxic SCA3 mutation carriers were characterized and quantified by magnetic resonance neurography (MRN).

Methods: Eighteen SCA3 mutation carriers and 20 age-/sex-matched healthy controls were prospectively enrolled. All SCA3 mutation carriers underwent detailed neurological and electrophysiological examinations. 3 T MRN covered the lumbosacral plexus and proximal thigh to the tibiotalar joint by using T2-weighted inversion recovery sequences, dual-echo relaxometry sequences with spectral fat saturation, and two gradient-echo sequences with and without an off-resonance saturation rapid frequency pulse. Detailed quantification of nerve lesions by morphometric and microstructural MRN markers, including T2 relaxometry and magnetization transfer contrast imaging, was conducted in all study participants.

Results: MRN detected peripheral nerve damage in ataxic and pre-ataxic SCA3. The quantitative markers proton spin density (ρ), T2 relaxation time, magnetization transfer ratio and cross-sectional area were decreased in SCA3, indicating chronic axonopathy. MTR and ρ identified early, subclinical nerve damage in pre-ataxic SCA3 and in SCA3 mutation carriers without polyneuropathy and were superior in differentiating between all subgroups. Additionally, microstructural markers correlated well with clinical symptom scores and electrophysiological results.

Conclusions: Our data provide a comprehensive characterization of peripheral nerve damage in SCA3 and assist in understanding the mechanisms of the multisystemic disease evolution. Evidence of peripheral nerve involvement prior to the onset of clinically overt ataxia might have important implications for designing early intervention studies.

KEYWORDS

electrophysiology, magnetic resonance neurography, polyneuropathy, quantitative imaging markers, spinocerebellar ataxia

This is an open access article under the terms of the [Creative Commons Attribution-NonCommercial-NoDerivs](https://creativecommons.org/licenses/by-nc-nd/4.0/) License, which permits use and distribution in any medium, provided the original work is properly cited, the use is non-commercial and no modifications or adaptations are made.

© 2022 The Authors. *European Journal of Neurology* published by John Wiley & Sons Ltd on behalf of European Academy of Neurology.

INTRODUCTION

Spinocerebellar ataxias (SCAs) are heterogeneous autosomal dominant inherited ataxic disorders leading to progressive disability and premature death. The most common subtype worldwide is spinocerebellar ataxia type 3 (SCA3) [1].

SCA3 affects not only the cerebellum but several regions of the nervous system such as the basal ganglia, brainstem, thalamus, spinal cord, dorsal root ganglia and peripheral nerves [2]. As SCA3 is caused by CAG trinucleotide repeat expansions in the *ATXN3* gene with full penetrance, pre-ataxic mutation carriers provide a unique opportunity to study early pathophysiological changes. Age at onset of SCA3 is mainly in the third or fourth decade but is highly variable, partly depending on the repeat length of the expanded allele [3]. Clinically, progressive ataxia is the most prominent feature [4], but the majority of SCA3 patients show clinical symptoms and electrophysiological evidence of an additional peripheral neuropathy with sensory disturbances, areflexia, weakness and muscle wasting [5,6].

In previous studies, magnetic resonance neurography (MRN) detected and localized peripheral nerve lesions in vivo at early, even presymptomatic disease stages in different diffuse neuropathies [7–10]. The aim of this explorative study was to characterize lower extremity peripheral nerve lesions by MRN in genetically, clinically and electrophysiologically classified pre-ataxic and ataxic SCA3 mutation carriers in comparison with healthy controls. To quantify peripheral nerve damage on a macroscopic and microstructural level, T2 relaxometry, magnetization transfer contrast (MTC) imaging and morphometric quantification were performed.

METHODS

Study design, neurological and electrophysiological assessments

This prospective case-control study was approved by the institutional ethics board (University of Heidelberg; S-398/2012), and all participants gave written informed consent.

Eighteen SCA3 mutation carriers (nine males, nine females, mean age 41.2 ± 2.9 years, range 22–64 years) and 20 age- and sex-matched healthy volunteers (10 males, 10 females, 41.4 ± 2.9 years, range 21–64 years) were enrolled from May 2017 to August 2020. Exclusion criteria were based on patients' past medical history and medical records, comprising age <18 years, pregnancy, concomitant causes of polyneuropathy (PNP) (diabetes mellitus, hypothyroidism, vitamin B12 deficiency), malignant or infectious diseases, neurological disorders other than SCA3, and contraindications for magnetic resonance imaging (MRI). Known exposure to environmental or occupational exogenous noxae, and previous treatment with chemotherapies, cytostatics or other potentially neurotoxic drugs were further exclusion criteria.

Severity of ataxia was assessed using the Scale for the Assessment and Rating of Ataxia (SARA) [11], whilst neurological signs other than ataxia (e.g., impaired vibration sense, tendon reflexes) were documented with the Inventory of Non-Ataxia Signs (INAS) [12]. Pallesthesia was graded as none (8/8), mild (5–7/8), moderate (2–5/8) or severe (<2/8). Mutation carriers were classified as either pre-ataxic or ataxic with manifest ataxia being defined by a SARA score of ≥ 3 [11].

The presence of PNP in our cohort was solely defined based on electroneurographic results, as clinical assessments may be influenced by potentially overlapping clinical symptoms originating from spinal cord or brain pathologies. For this purpose, motor nerve conduction studies assessed distal motor latencies, compound muscle action potentials (CMAPs) and nerve conduction velocities (NCVs) of the right peroneal and left tibial nerves. Sensory nerve action potentials (SNAPs) and NCVs were measured for the right and left sural nerves (G.S., M.W.; Natus, Keypoint G4, Version 2.4). Skin temperature was controlled at a minimum of 32°C. PNP was diagnosed when either CMAP or SNAP amplitudes were pathological in at least two different leg nerves, according to in-house validated reference parameters, after exclusion of focal entrapment neuropathies and innervation variants.

For pre-ataxic mutation carriers, the predicted age of ataxia onset was calculated based on the CAG repeat length [13].

Magnetic resonance neurography protocol

All participants underwent the following high-resolution MRN protocol in a 3.0 T MR scanner (Magnetom PRISMA, Siemens-Healthineers).

1. 3D T2-weighted inversion recovery SPACE (sampling perfection with application-optimized contrasts using different flip angle evolution) sequence was carried out for imaging the lumbar plexus and spinal nerves with 50 axial reformations per patient: repetition time (TR)/echo time (TE)/inversion time 3000/205/210 ms, field-of-view (FoV) $305 \times 305 \text{ mm}^2$, matrix size $320 \times 320 \times 104$, slice thickness 1.0 mm, no gap, voxel size $1.0 \times 1.0 \times 1.0 \text{ mm}^3$, acquisition time 8:35 min.
2. Axial dual-echo turbo-spin-echo 2D sequences with spectral fat saturation were carried out for T2 relaxometry with four continuous slabs at the left leg: slab1, proximal thigh to mid-thigh; slab2, mid-thigh to distal thigh with alignment of the distal edge of this imaging slab on the tibiofemoral joint space; slab3, lower leg with alignment of its proximal edge with the tibiofemoral joint space; slab4, ankle level with alignment of the distal edge on the tibiotalar joint space. One additional slab was acquired at the right mid to distal thigh. Sequence parameters were TR 5860 ms, TE₁ 14 ms, TE₂ 86 ms, FoV $170 \times 170 \text{ mm}^2$, matrix size 512×512 , slice thickness 3.5 mm, interslice gap 0.35 mm, voxel size $0.3 \times 0.3 \times 3.5 \text{ mm}^3$, flip angle 180°, 35 slices, acquisition time per slab 8:25 min.

- Two axial three-dimensional, gradient-echo sequences with and without an off-resonance saturation pulse (Gaussian envelope, duration 9984 μ s, frequency offset 1200 Hz) were carried out at the exact same slice position at the right mid to distal thigh: TR 50 ms, TE 4.92 ms, FoV 160 \times 160 mm², matrix size 256 \times 256, bandwidth 370 Hz/Px, slice thickness 3.5 mm, voxel size 0.6 \times 0.6 \times 3.5 mm³, flip angle 7°, 16 slices, acquisition time per sequence 3:48 min.

The net acquisition time including survey scans was 61:35 min. Patient and coil repositioning required an additional 20–30 min. An 18-channel body-array flex-coil (Siemens-Healthineers) was used for imaging of the lumbar plexus (sequence (1)), and a 15-channel transmit-receive extremity coil (INVIVO) for imaging of the left and right leg (sequences (2) and (3)).

Image post-processing and analyses

All images were analyzed in ImageJ (version 1.52v; National Institutes of Health). Tibial fascicles of the left sciatic nerve and their distal continuation as tibial nerve with coverage from the proximal thigh down to the distal ankle were segmented on 140 axial slices/participant generated by sequence (2) by one neuroradiologist (J.K.) blinded to clinical data. To exclude significant side differences, the tibial nerve was additionally segmented on 35 axial slices at the right mid to distal thigh, a region where previous studies predominantly identified nerve lesions in different neuropathies [7,14–16].

For the same reason, MTC imaging was performed at the distal thigh. To avoid any potential inaccuracies in identifying tibial or peroneal fascicles due to the lower resolution of MTC sequences, it was decided to segment the whole sciatic nerve on 10 consecutive slices at the center of sequence (3), approximately 1 cm proximal to the nerve bifurcation (J.K.).

Signal quantification

The apparent T2 relaxation time (T_{2app} , Equation 1) and proton spin density (ρ , Equation 2) were calculated by using relaxometry data (sequence (2)) with TE₁ set at 14 ms and TE₂ set at 86 ms [17].

$$T_{2app} = \frac{TE_2 - TE_1}{\ln[SI(TE_1)/SI(TE_2)]} \quad (1)$$

$$\rho = \frac{SI(TE_1)}{\exp(TE_1/T_{2app})} \quad (2)$$

Mean values of nerve ρ and T_{2app} were calculated per slice position for each participant. Subsequently, averaged mean ρ and T_{2app} values of the tibial nerve at the thigh (imaging slabs 1 and 2) were compared to respective mean values of the lower leg (imaging slabs 3 and 4) to test for potential location-dependent differences along the

proximal-to-distal course of the tibial nerve. Further analyses were conducted to test for differences between subgroups (SCA3, SCA3 with PNP (SCA3 PNP+), SCA3 without PNP (SCA3 PNP-), pre-ataxic mutation carriers, controls).

Magnetization transfer contrast imaging

The magnetization transfer ratio (MTR) was calculated separately for each participant and each evaluated axial imaging slice according to the following equation, in which S_0 is the signal without and S_1 with off-resonance saturation:

$$MTR = 100 \times \frac{S_0 - S_1}{S_0}$$

MTR values were subsequently extracted from each slice position and averaged over all slice positions for each participant. Computed sciatic nerve MTR mean values were then compared between the different groups.

Morphometric quantification

Tibial nerve caliber was measured as cross-sectional area (CSA) on each axial slice for morphometric quantification. Bilateral proximal spinal nerves L5 and S1 were additionally segmented on axial reformations of sequence (1). The lumbosacral plexus was segmented at the level of the sciatic notch on both sides.

Statistical analyses

Statistical data analyses were performed in GraphPad Prism 9.0.2 (J.K., J.M.H.). Differences between SCA3 and controls, pre-ataxic mutation carriers and controls, the left and right distal thigh, and the thigh and the lower leg were evaluated with the Mann-Whitney test. Subgroup analyses between SCA3 PNP+, SCA3 PNP-, and controls were performed by using a one-way ANOVA for a priori assumptions. Subsequent post hoc analyses were corrected for multiple comparisons by using the Tukey-Kramer test. Pearson's correlation coefficients were calculated for correlation analyses between MRN parameters and demographic (age, sex, height, weight, body mass index), clinical (duration of symptoms, SARA, INAS, pallesthesia, CAG expanded and normal allele), and electrophysiological (tibial and peroneal NCV, distal motor latencies, CMAP, and sural nerve NCV and SNAP) results. Statistical tests were two-tailed and an alpha level of significance was defined at $p < 0.05$. All results are documented as mean values \pm SEM.

All data used to conduct this study are documented in the Methods section. Additional anonymized datasets will be shared on request from any qualified investigator.

RESULTS

Clinical and electrophysiological data

Seven of the 18 SCA3 mutation carriers were classified as pre-ataxic defined by a SARA score of <3. Six of the 11 ataxic and none of the pre-ataxic mutation carriers fulfilled the electrophysiological criteria for PNP. There were no differences with respect to the CAG repeat length of the mutated allele, but SCA3 PNP+ showed an older age, higher SARA scores and higher INAS counts (Table 1). The mean predicted age of ataxia onset in pre-ataxic mutation carriers calculated

on the basis of the CAG repeat length was -4.89 years. Detailed demographic and clinical characteristics are given in Table 1.

Magnetic resonance neurography data

Proton spin density

Tibial nerve ρ was markedly decreased in SCA3 (390.8 ± 14.5 a.u.) versus controls (472.8 ± 10.4 a.u.; $p < 0.0001$; Figure 1a) at the thigh and at the lower leg (SCA3 384.0 ± 14.6 a.u. vs. controls

TABLE 1 Demographic, clinical and electrophysiological data

Parameter	SCA3 (n = 18)	SCA3 PNP+ (n = 6)	SCA3 PNP- (n = 12)	p value SCA3 PNP+ versus SCA3 PNP-
Age (years)	42.3 \pm 3.0	54.7 \pm 2.7	36.1 \pm 2.9	0.0069*
Sex (m/f)	9/9	4/2	5/7	n.a.
Body weight (kg)	74.2 \pm 2.8	80.0 \pm 2.3	71.3 \pm 3.8	0.20 (ns)
Height (cm)	1.75 \pm 0.02	1.76 \pm 0.05	1.75 \pm 0.03	0.57 (ns)
Body mass index (kg/m ²)	24.2 \pm 0.8	26.1 \pm 1.5	23.2 \pm 0.9	0.35 (ns)
CAG long allele	68.7 \pm 0.9	67.5 \pm 0.4	69.3 \pm 1.4	0.29 (ns)
CAG short allele	25.3 \pm 3.1	28.4 \pm 8.1	23.4 \pm 1.6	0.65 (ns)
SARA (0–40 points)	7.86 \pm 1.72	15.25 \pm 2.89	4.17 \pm 1.09	0.0005***
INAS (0–16 points)	2.83 \pm 0.51	5.33 \pm 0.67	1.58 \pm 0.29	<0.0001***
PTR areflexia/normal/hyperreflexia	4/12/2	3/3/0	1/9/2	n.a.
ATR areflexia/normal/hyperreflexia	7/9/2	5/1/0	2/8/2	n.a.
Pallhypesthesia (none/mild/moderate/severe)	3/9/4/2	0/0/4/2	3/9/0/0	n.a.
Disease stage (0/1/2/3)	7/9/1/1	0/4/1/1	7/5/0/0	n.a.
SNAP (μ V)				
RSN	10.1 \pm 1.6	3.4 \pm 0.9	12.9 \pm 1.6	0.0005***
LSN	8.4 \pm 1.5	3.0 \pm 0.7	10.9 \pm 1.7	0.0009***
CMAP (mV)				
RPN	5.9 \pm 0.8	3.3 \pm 1.2	7.2 \pm 0.9	0.0105*
LTN	17.4 \pm 2.1	9.2 \pm 2.7	21.6 \pm 2.1	0.0065*
DML (ms)				
RPN	4.4 \pm 0.2	5.0 \pm 0.6	4.1 \pm 0.2	0.10 (ns)
LTN	3.8 \pm 0.1	3.7 \pm 0.1	3.8 \pm 0.1	0.84 (ns)
NCV (m/s)				
RPN	45.9 \pm 1.1	42.2 \pm 1.9	47.8 \pm 1.1	0.0163*
LTN	47.3 \pm 0.8	45.5 \pm 1.4	48.1 \pm 1.0	0.11 (ns)
RSN	49.4 \pm 1.2	46.8 \pm 2.5	50.5 \pm 1.2	0.22 (ns)
LSN	48.2 \pm 1.4	45.0 \pm 2.1	49.6 \pm 1.6	0.10 (ns)

Note: All results are presented as mean values \pm standard error of the mean.

Abbreviations: ATR, Achilles tendon reflex; CMAP, compound muscle action potential; DML, distal motor latency; INAS, Inventory of Non-Ataxia Signs; LSN, left sural nerve; LTN, left tibial nerve; NCV, nerve conduction velocity; ns, not significant; PTR, patellar tendon reflex; RPN, right peroneal nerve; RSN, right sural nerve; SARA, Scale of the Assessment and Rating of Ataxia; SCA3, spinocerebellar ataxia type 3 mutation carrier; SCA3 PNP-, SCA3 mutation carriers without polyneuropathy; SCA3 PNP+, SCA3 mutation carriers with polyneuropathy; SNAP, sensory nerve action potential.

Disease stage 0, no gait problems; 1, ataxic, do not need a walking aid; 2, permanently using a walking aid; 3, wheelchair bound. Pallhypesthesia: none, 8/8; mild, >5/8; moderate, 2–5/8; severe, <2/8.

*Significant ($p \leq 0.05$).

***Highly significant ($p \leq 0.001$).

449.4 ± 13.9 a.u.; $p = 0.0013$). When subdividing the SCA3 group into SCA3 PNP+ and SCA3 PNP-, group differences were identified at the thigh ($p < 0.0001$, $F = 11.98$) and at the lower leg ($p = 0.0013$; $F = 7.440$). Subsequent post hoc analyses revealed that nerve ρ at the thigh was lower in SCA3 PNP+ (362.7 ± 16.2 a.u.; $p = 0.0002$) and in SCA3 PNP- (403.1 ± 19.2 a.u.; $p = 0.0018$) versus controls, but differences between the two SCA3 groups did not exist ($p = 0.31$; Figure 1a and 2). At the lower leg, ρ was only lower in SCA3 PNP+ (339.54 ± 20.2 a.u.; $p = 0.0013$) versus controls. Furthermore, a decrease in tibial nerve ρ was already found in pre-ataxic SCA3 (thigh, 392.7 ± 26.7 a.u.; lower leg, 397.5 ± 25.2 a.u.) versus controls (thigh, $p = 0.0016$, Figure 1a; lower leg, $p = 0.0442$). A proximal-to-distal gradient or a difference between the left and right thigh was absent in SCA3 and controls ($p > 0.05$).

An inverse correlation was identified between tibial nerve ρ at the thigh and the SARA ($r = -0.45$, $p = 0.0093$) and INAS score ($r = -0.40$, $p = 0.0219$). Consistent correlations between tibial nerve ρ at the thigh or lower leg level and any of the remaining demographic, clinical or electrophysiological parameters did not exist.

Apparent T2 relaxation time

Tibial nerve T2_{app} at thigh level was lower in SCA3 (63.9 ± 0.9 ms) than in controls (67.1 ± 0.8 ms; $p = 0.0137$; Figure 1b and 2) and was also decreased at the lower leg in SCA3 (61.1 ± 1.1 ms) versus controls (64.9 ± 1.1 ms; $p = 0.0136$). ANOVA indicated subgroup differences at the thigh ($p = 0.0082$; $F = 5.180$) but not at the lower leg ($p = 0.06$; $F = 2.943$). In detail, T2_{app} at the thigh was lower in SCA3 PNP+ (61.9 ± 1.3 ms) versus controls ($p = 0.0093$), whilst no differences existed between SCA3 PNP- (64.7 ± 1.1 ms) and controls ($p = 0.14$) or between SCA3 PNP+ and SCA3 PNP- ($p = 0.28$; Figure 1b). Differences in T2_{app} between pre-ataxic SCA3 (thigh, 64.6 ± 1.5 ms; lower leg, 61.9 ± 1.3 ms) and controls were not observed (thigh, $p = 0.16$, Figure 1b; lower leg, $p = 0.15$). A slight proximal-to-distal gradient in T2_{app} was found in SCA3 ($p = 0.0268$) and controls ($p = 0.0428$). Side differences did not exist in SCA3 or controls ($p > 0.05$).

Correlation analyses revealed an inverse correlation between tibial nerve T2_{app} at thigh level and the INAS ($r = -0.47$, $p = 0.0055$) and positive correlations with peroneal CMAPs ($r = 0.52$, $p = 0.0017$), tibial NCVs ($r = 0.38$, $p = 0.0310$) and sural SNAPs ($r = 0.53$, $p = 0.0029$). At the lower leg, tibial nerve T2_{app} correlated with peroneal CMAPs ($r = 0.37$, $p = 0.0317$) and sural SNAPs ($r = 0.36$, $p = 0.0452$).

Magnetization transfer ratio

Sciatic nerve MTR was clearly reduced in SCA3 (28.1% ± 0.5%) versus controls (33.0% ± 0.5%, $p < 0.0001$; Figure 1c). ANOVA revealed marked differences between SCA3 PNP+, SCA3 PNP- and controls ($p < 0.0001$; $F = 32.78$). In detail, MTR values were

lower in SCA3 PNP+ (25.9% ± 0.9%, $p < 0.0001$) and SCA3 PNP- (29.2% ± 0.4%, $p < 0.0001$) versus controls, and were also lower in SCA3 PNP+ versus SCA3 PNP- ($p = 0.0094$; Figures 1c and 3). Additional analyses showed that the MTR was already decreased in pre-ataxic SCA3 (29.7% ± 0.5%) versus controls ($p = 0.0006$; Figure 1c).

Sciatic nerve MTR showed an inverse correlation with age ($r = -0.71$, $p = 0.0028$), but not with other demographic parameters. Inverse correlations were found between MTR and disease duration ($r = -0.62$, $p = 0.0097$), SARA ($r = -0.57$, $p = 0.0225$), INAS ($r = -0.60$, $p = 0.0146$) and pallesthesia ($r = -0.5103$, $p = 0.0434$). MTR also correlated well with peroneal ($r = 0.65$, $p = 0.0063$) and tibial NCV ($r = 0.73$, $p = 0.0068$) as well with peroneal ($r = 0.61$, $p = 0.0254$) and tibial CMAPs ($r = 0.72$, $p = 0.0016$) and sural SNAPs (right, $r = 0.71$, $p = 0.0031$; left, $r = 0.69$, $p = 0.0067$).

Cross-sectional area

The cross-sectional area (CSA) of the tibial nerve was markedly lower in SCA3 (12.1 ± 0.3 mm²) versus controls (14.2 ± 0.3 mm²; $p < 0.0001$; Figure 1d) at the thigh and at the lower leg (SCA3 6.3 ± 0.3 mm² vs. controls 7.2 ± 0.2 mm²; $p = 0.0181$). Differences between subgroups were detected at the thigh ($p < 0.0001$; $F = 11.58$) but not at the lower leg ($p = 0.06$; $F = 3.020$). At the thigh, CSA was decreased in SCA3 PNP+ (12.5 ± 1.0 mm²; $p = 0.0361$) and SCA3 PNP- (11.9 ± 0.3 mm²; $p < 0.0001$) versus controls, whilst no CSA differences were detected between the two SCA3 subgroups ($p = 0.63$; Figure 1d and 2). Tibial nerve CSA was also different between controls and pre-ataxic SCA3 (12.1 ± 0.3 mm²; $p = 0.0003$; Figure 1d) at the thigh but not at the lower leg ($p = 0.07$). Consistent with the physiological decrease in nerve caliber, tibial nerve CSA was markedly higher at the thigh than at the lower leg in SCA3 and controls ($p < 0.0001$, respectively). Side differences between right and left tibial nerve CSAs were not observed in SCA3 or controls ($p > 0.05$).

Tibial nerve CSA at thigh level correlated positively with patient weight ($r = 0.43$, $p = 0.0164$) and body mass index ($r = 0.36$, $p = 0.0447$). No further consistent correlations were found between tibial nerve CSA and any of the remaining evaluated parameters.

Analyses of proximal spinal nerves and the lumbosacral plexus revealed no differences in CSA between SCA3 (L5, 3.9 ± 0.2 mm²; S1, 4.0 ± 0.2 mm²; plexus, 7.4 ± 0.4 mm²) and controls (L5, 3.8 ± 0.3 mm², $p = 0.53$; S1, 3.7 ± 0.2 mm², $p = 0.21$; plexus, 8.0 ± 0.5 mm², $p = 0.33$). Therefore, no further analyses were performed in the SCA3 subgroups.

DISCUSSION

SCA3 is a multisystemic disease that affects different anatomical regions within the central nervous system and the peripheral nervous system, frequently leading to central neurological symptoms and

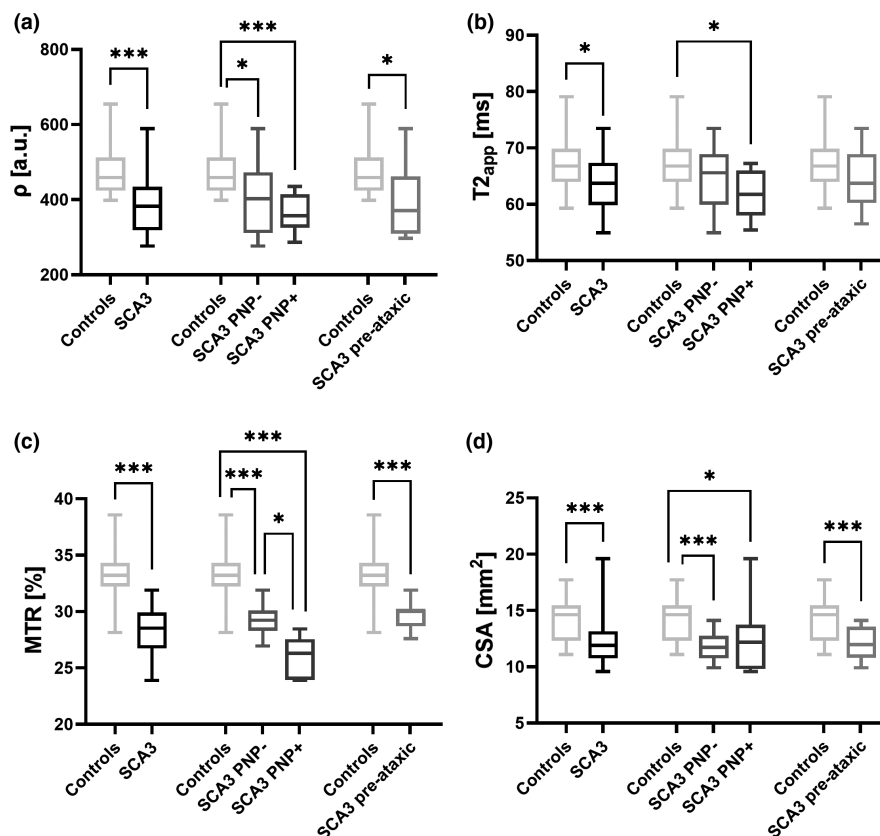


FIGURE 1 Quantitative MRN markers. Nerve ρ (a), $T2_{app}$ (b), MTR (c) and CSA (d) mean values at thigh level were plotted separately for each group in a box and whisker plot. All quantitative markers differentiated well between healthy controls and all SCA3 mutation carriers by a significant decrease. In addition, ρ , MTR and CSA separated SCA3 mutation carriers without electrophysiologically manifest polyneuropathy (PNP) as well as pre-ataxic SCA3 mutation carriers from controls, whilst $T2_{app}$ only identified SCA3 patients with manifest PNP. Further differentiation between SCA3 mutation carriers with and without PNP was only possible by analyzing sciatic nerve MTR. CSA, cross-sectional area; MTR, magnetization transfer ratio; SCA3, spinocerebellar ataxia type 3 mutation carrier; SCA3 PNP-, SCA3 mutation carriers without polyneuropathy; SCA3 PNP+, SCA3 mutation carriers with polyneuropathy; $T2_{app}$, apparent T2 relaxation time; ρ , proton spin density. Significant differences are indicated by either *significant ($p \leq 0.05$) or ***highly significant ($p \leq 0.001$)

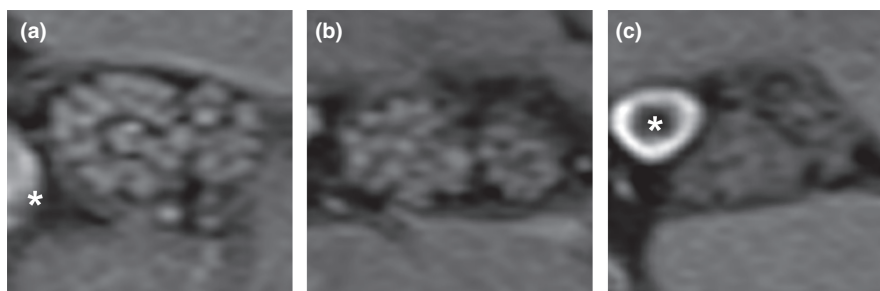


FIGURE 2 Magnetic resonance neurography (MRN) source images. Representative MRN images (axial dual-echo turbo-spin-echo relaxometry sequences with spectral fat saturation) at left mid-thigh level are shown at equal slice positions in a healthy control (a), an SCA3 mutation carrier without polyneuropathy (PNP) (b) and an SCA3 mutation carrier with PNP (c). Details show the tibial and peroneal fascicles within the sciatic nerve. Note the slight decrease in sciatic nerve T2-weighted signal, a consequence of the decrease in both ρ and $T2_{app}$, and sciatic nerve CSA in SCA3 PNP- (b) and in SCA3 PNP+ (c) compared to the healthy control (a). * indicates perineural vessels

signs of peripheral neuropathy [2,4,6]. Knowledge about the exact mechanisms preceding disease onset and leading to disease progression is limited.

Here, the first comprehensive characterization and quantification of peripheral nerve involvement in pre-ataxic and ataxic

SCA3 mutation carriers by applying quantitative MRN is reported. Our results show that (i) all evaluated microstructural and morphometrical quantitative MRN parameters are markedly decreased in SCA3 compared to controls, (ii) nerve impairment is also detectable in pre-ataxic mutation carriers and in SCA3 patients without PNP,

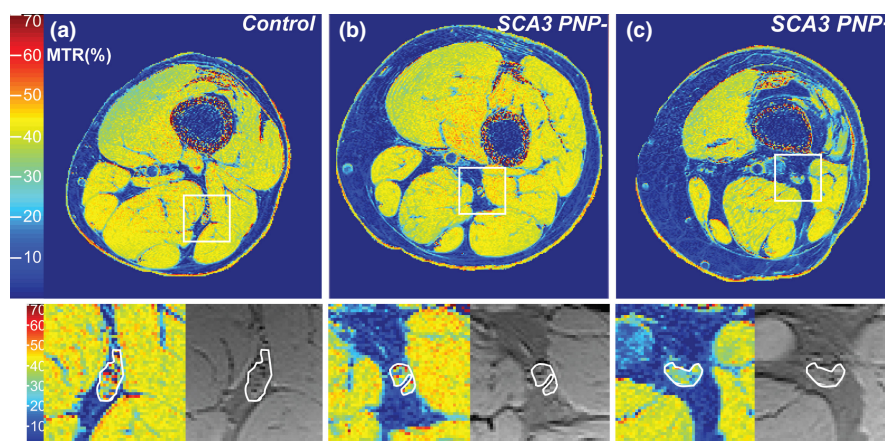


FIGURE 3 Magnetization transfer ratio map. Representative MTR pseudo-colored (%) maps are shown for a healthy control (a), an SCA3 mutation carrier without polyneuropathy (PNP) (b) and an SCA3 mutation carrier with PNP (c). The white boxes in (a)–(c) are zoomed-in and displayed below to show detailed views of the MTR (%) map (left) and the MTC sequence without the off-resonance pulse (right) with the sciatic nerve at the left mid-thigh encircled in white. Note the marked decrease of sciatic nerve MTR (%) in SCA3 PNP– ((b), loss of red and yellow signals), and even further decrease in SCA3 PNP+ (c) compared to the healthy control (a) [Colour figure can be viewed at [wileyonlinelibrary.com](https://onlinelibrary.wiley.com)]

and (iii) ρ and MTR are the most suitable MRN markers to allow an early diagnosis and differentiation between subgroups whilst correlating well with disease severity.

ρ and T_{2app} are known to be microstructural markers of nerve tissue integrity in vivo, depending on the macromolecular composition of nerve tissue [17–19]. Both markers were recently established for the quantification of nerve lesions in various peripheral nervous system diseases by our group and have become increasingly important on the path to developing imaging biomarkers [7,9,15,20,21]. Recent studies consistently concluded that typical, distal-symmetric PNPs of different etiologies are characterized by an early increase of ρ , followed by an additional increase in T_{2app} in symptomatic PNP [7,9,15,22]. In contrast, nerve injury in 5q-linked spinal muscular atrophy (SMA), as an example for a neurodegenerative motor neuron disease, was characterized by a decrease in ρ (opposite to results in PNPs) and an increase in T_{2app} (similar to results in PNPs) [8], whilst peripheral nerve involvement in multiple sclerosis (MS), as an example of a demyelinating disease, showed an increase in ρ (similar to results in PNPs) and a decrease in T_{2app} (opposite to results in PNPs) [21].

Our finding of a combined decrease in ρ and T_{2app} in SCA3 is unique amongst the multitude of diffuse neuropathies investigated by MRN so far, representing a different pathomechanism of peripheral neuropathy in SCA3. Electrophysiologically, peripheral nerve involvement in SCA3 presents as a pure axonal neuropathy with sensory or sensorimotor symptoms, partially accompanied by fasciculations [23,24]. The axonal damage in SCA3 is a likely explanation for the observed decrease of ρ in SCA3. It has been similarly described in SMA where the decay of lower motor neurons with subsequent axonal loss is the predominant pathomorphological hallmark [8]. However, the reactive increase in T_{2app} detected in SMA, hypothetically induced by nerve edema, was absent in our SCA3 cohort. The decrease of nerve ρ in our study points against demyelination

as a relevant factor in the development of peripheral neuropathy in SCA3. Areas of increased ρ in the brain of deceased MS patients were previously histopathologically correlated with areas of demyelination [25], and in a recent MRN study conducted in MS patients, peripheral nerve lesions were associated with an increase in ρ , leading to the hypothesis of a peripheral co-demyelination [21]. In SCA3, additional demyelinating components are uncommon and would rather point towards SCA mimicking immunological or neurometabolic diseases [24]. Instead, the additional decrease in tibial nerve CSA indicates neuronal atrophy, further supporting the hypothesis of a chronic degenerative process in SCA3 characterized by predominant axonal loss.

MTC imaging provides additional information on the concentration of protons bound to macromolecules that cannot be directly measured by conventional MRI sequences and their interaction with free water molecules [26–29]. The first study applying MTC imaging in neuropathic patients was conducted in Charcot–Marie–Tooth disease type 1A, where MTR correlated well with the grade of disability [30]. These promising results were recently confirmed in hereditary transthyretin amyloidosis, where MTR correlated well with clinical PNP symptom scores and electrophysiological results and detected early nerve damage in clinically and electrophysiologically completely asymptomatic carriers of the variant *transthyretin* gene [31]. In initial studies, it was assumed that an MTR decrease indicates the degree of demyelination, but other studies favored a reduced axonal density as the origin for a reduced MTR [26]. The latter hypothesis was supported by the finding of decreased nerve MTR values in SMA, where axonal loss accounts for the predominant pathomorphological fingerprint [32] and is probably the underlying reason for the MTR decrease observed in our SCA3 cohort. Moreover, sciatic nerve MTR was the sole MRN marker that differentiated SCA3 PNP– not only from healthy controls (similar to ρ , T_{2app} and CSA) but also from SCA3 PNP+. Even though MTR decreases in pathophysiologically completely different disease entities

like Charcot–Marie–Tooth disease type 1A, hereditary transthyretin amyloidosis, SMA and SCA3, making it an unspecific MRN marker, it might be the most promising and sensitive biomarker to differentiate between SCA3 subgroups and to detect early nerve injury in pre-ataxic and SCA3 PNP– mutation carriers.

In our study cohort, six of the 11 ataxic and none of the pre-ataxic SCA3 mutation carriers fulfilled the electrophysiological criteria for PNP. Conversely, quantitative MRN markers, especially MTR, showed a gradual decrease from controls over SCA3 PNP– to SCA3 PNP+, and from controls to pre-ataxic SCA3. In particular, our finding of a significant decrease in ρ , MTR and CSA in pre-ataxic SCA3 mutation carriers indicates that—even without electrophysiological signs of PNP—mild peripheral nerve involvement is already present in the pre-ataxic stage but remains clinically inapparent until a certain threshold is exceeded.

Quantitative MRN markers correlated well with the SARA, INAS and electrophysiological results but are more objective and observer independent compared to clinical rating scales, making quantitative MRN markers promising supportive tools for monitoring disease progression in the future.

The cross-sectional design of our study does not allow an interpretation regarding the temporal progression of structural nerve damage. Future longitudinal studies assessing MRN in correlation with clinical and electrophysiological disease progression would be desirable and are part of ongoing follow-up examinations. This approach will prove whether quantitative MRN parameters can be used as progression biomarkers in clinical trials. Here, the acquisition time for the MRN protocol may be markedly reduced by limiting the recording of quantitative data to one leg and one anatomical location. Future studies should also test the potential of high-resolution nerve ultrasound to detect peripheral nerve lesions in SCA3, as ultrasound might be more broadly available than MRN. Another limitation is the small number of participants. However, our focus was on SCA3, the most common SCA subtype, for our exploratory study as recruitment of a sufficiently large number of mutation carriers of all other genotypes was not feasible at our center.

Our study results provide comprehensive data on the *in vivo* characterization of peripheral nerve damage in SCA3 that contributes towards an understanding of the mechanisms behind the multisystemic disease evolution. Whilst all analyzed MRN markers differentiated well between healthy controls and SCA3 mutation carriers, ρ and MTR are most suited to differentiate between SCA3 subgroups and to identify pre-ataxic and SCA3 PNP– mutation carriers. The identification of peripheral nerve involvement in pre-ataxic SCA3 mutation carriers by MRN as an early sign of disease manifestation might have important implications for the planning of future preventive clinical trials as therapeutic strategies might target SCA3 mutation carriers prior to the onset of clinically manifest ataxia and before irreversible brain damage occurs.

ACKNOWLEDGEMENTS

The authors thank Gustav Neitz, Department of Neuroradiology, Heidelberg University Hospital, for scheduling patient appointments. Open access funding enabled and organized by ProjektDEAL.

CONFLICT OF INTEREST

J. Kollmer received a research grant, personal fees, lecture honoraria and financial support for conference attendance from Alnylam Pharmaceuticals, the Olympia Morata stipend grant from the Medical Faculty of the University of Heidelberg, lecture honoraria and financial support for conference attendance from Pfizer, and advises for Akcea Therapeutics. M. Weiler advises for Akcea Therapeutics, Alnylam Pharmaceuticals, Biogen, Pfizer, Roche and Sobi, received lecture honoraria from Akcea Therapeutics, Alnylam Pharmaceuticals, Biogen and Roche, and received financial support for conference attendance from Biogen and Pfizer. G. Sam reports no disclosures relevant to this work. J. Faber received funding from the National Ataxia Foundation (NAF) and is a fellow of the Hertie Academy for Clinical Neuroscience. J.M. Hayes reports no disclosures relevant to this work. S. Heiland received research grants from the German Research Foundation (SFB 1118) and from the Dietmar Hopp Foundation. M. Bendszus reports personal fees from Boehringer Ingelheim, grants and personal fees from Novartis and Guerbet, grants from Siemens, the Hopp Foundation, the German Research Foundation (SFB 1158), the European Union and Stryker, personal fees from Merck, Bayer, Teva, BBraun, Vascular Dynamics, Grifols and Neuroscios. W. Wick reports no disclosures relevant to this work. H. Jacobi received the Olympia Morata stipend grant from the Medical Faculty of the University of Heidelberg.

AUTHOR CONTRIBUTIONS

Jennifer Kollmer: Conceptualization (lead); data curation (lead); formal analysis (lead); funding acquisition (equal); investigation (lead); methodology (lead); project administration (equal); resources (equal); software (equal); supervision (equal); validation (equal); visualization (equal); writing—original draft (lead); writing—review and editing (equal). Markus Weiler: Data curation (equal); investigation (equal); methodology (equal); validation (equal); writing—review and editing (equal). Georges Sam: Data curation (equal); investigation (supporting); writing—review and editing (equal). Jennifer Faber: Data curation (supporting); writing—review and editing (equal). John Hayes: Data curation (supporting); formal analysis (supporting); methodology (supporting); visualization (equal); writing—review and editing (equal). Sabine Heiland: Data curation (supporting); formal analysis (supporting); funding acquisition (equal); investigation (equal); methodology (equal); writing—review and editing (equal). Martin Bendszus: Data curation (supporting); funding acquisition (equal); investigation (equal); methodology (supporting); validation (supporting); writing—review and editing (equal). W. Wick: Data curation (supporting); investigation (supporting); methodology (supporting); validation (supporting); writing—review and editing (equal). Heike Jacobi: Conceptualization (lead); data curation (lead); formal analysis (equal); funding acquisition (equal); investigation (lead); methodology (equal); project administration (equal); resources (equal); supervision (equal); validation (equal); writing—original draft (lead); writing—review and editing (equal).

DATA AVAILABILITY STATEMENT

All data used to conduct this study are documented in the Methods section. Additional anonymized datasets will be shared on request from any qualified investigator.

ORCID

Jennifer Kollmer  <https://orcid.org/0000-0002-6254-9192>

Markus Weiler  <https://orcid.org/0000-0002-8942-7662>

REFERENCES

1. Ruano L, Melo C, Silva MC, Coutinho P. The global epidemiology of hereditary ataxia and spastic paraplegia: a systematic review of prevalence studies. *Neuroepidemiology*. 2014;42(3):174-183.
2. Koeppen AH. The neuropathology of spinocerebellar ataxia type 3/Machado-Joseph disease. In: Nobrega C, Pereira de Almeida L, eds. *Polyglutamine Disorders Advances in Experimental Medicine and Biology*. 1049: Springer; 2018.
3. Klockgether T, Mariotti C, Paulson HL. Spinocerebellar ataxia. *Nat Rev Dis Primers*. 2019;5(1):24.
4. Mendonca N, Franca MC Jr, Goncalves AF, Januario C. Clinical features of Machado-Joseph disease. *Adv Exp Med Biol*. 2018;1049:255-273.
5. van de Warrenburg BP, Notermans NC, Schelhaas HJ, et al. Peripheral nerve involvement in spinocerebellar ataxias. *Arch Neurol*. 2004;61(2):257-261.
6. Schmitz-Hubsch T, Coudert M, Bauer P, et al. Spinocerebellar ataxia types 1, 2, 3, and 6: disease severity and nonataxia symptoms. *Neurology*. 2008;71(13):982-989.
7. Kollmer J, Hund E, Hornung B, et al. In vivo detection of nerve injury in familial amyloid polyneuropathy by magnetic resonance neurography. *Brain*. 2015;138(Pt 3):549-562.
8. Kollmer J, Hilgenfeld T, Ziegler A, et al. Quantitative MR neurography biomarkers in 5q-linked spinal muscular atrophy. *Neurology*. 2019;93(7):e653-e664.
9. Pham M, Oikonomou D, Hornung B, et al. Magnetic resonance neurography detects diabetic neuropathy early and with proximal predominance. *Ann Neurol*. 2015;78(6):939-948.
10. Jende JME, Groener JB, Oikonomou D, et al. Diabetic neuropathy differs between type 1 and type 2 diabetes: insights from magnetic resonance neurography. *Ann Neurol*. 2018;83(3):588-598.
11. Schmitz-Hubsch T, du Montcel ST, Baliko L, et al. Scale for the assessment and rating of ataxia: development of a new clinical scale. *Neurology*. 2006;66(11):1717-1720.
12. Jacobi H, Rakowicz M, Rola R, et al. Inventory of Non-Ataxia Signs (INAS): validation of a new clinical assessment instrument. *Cerebellum*. 2013;12(3):418-428.
13. Tezenas du Montcel S, Durr A, Rakowicz M, et al. Prediction of the age at onset in spinocerebellar ataxia type 1, 2, 3 and 6. *J Med Genet*. 2014;51(7):479-486.
14. Rother C, Bumb JM, Weiler M, et al. Characterization and quantification of alcohol-related polyneuropathy by magnetic resonance neurography. *Eur J Neurol*. 2022;29(2):573-582.
15. Kollmer J, Weiler M, Purucker J, et al. MR neurography biomarkers to characterize peripheral neuropathy in AL amyloidosis. *Neurology*. 2018;91(7):e625-e634.
16. Kollmer J, Bendszus M. Magnetic resonance neurography: improved diagnosis of peripheral neuropathies. *Neurotherapeutics*. 2021;18(4):2368-2383.
17. Heiland S, Sartor K, Martin E, Bardenheuer HJ, Plaschke K. In vivo monitoring of age-related changes in rat brain using quantitative diffusion magnetic resonance imaging and magnetic resonance relaxometry. *Neurosci Lett*. 2002;334(3):157-160.
18. Miot E, Hoffschir D, Alapetite C, et al. Experimental MR study of cerebral radiation injury: quantitative T2 changes over time and histopathologic correlation. *AJNR Am J Neuroradiol*. 1995;16(1):79-85.
19. Walimuni IS, Hasan KM. Atlas-based investigation of human brain tissue microstructural spatial heterogeneity and interplay between transverse relaxation time and radial diffusivity. *NeuroImage*. 2011;57(4):1402-1410.
20. Kollmer J, Sahm F, Hegenbart U, et al. Sural nerve injury in familial amyloid polyneuropathy: MR neurography vs clinicopathologic tools. *Neurology*. 2017;89(5):475-484.
21. Jende JME, Hauck GH, Diem R, et al. Peripheral nerve involvement in multiple sclerosis: demonstration by magnetic resonance neurography. *Ann Neurol*. 2017;82(5):676-685.
22. Rother C, Bumb JM, Weiler M, et al. Characterization and quantification of alcohol-related polyneuropathy by magnetic resonance neurography. *Eur J Neurol*. 2022;29(2):573-582.
23. Berciano J, Infante J, Garcia A, et al. Stiff man-like syndrome and generalized myokymia in spinocerebellar ataxia type 3. *Mov Disord*. 2006;21(7):1031-1035.
24. Schols L, Linnemann C, Globas C. Electrophysiology in spinocerebellar ataxias: spread of disease and characteristic findings. *Cerebellum*. 2008;7(2):198-203.
25. Nijeholt GJ, Bergers E, Kamphorst W, et al. Post-mortem high-resolution MRI of the spinal cord in multiple sclerosis: a correlative study with conventional MRI, histopathology and clinical phenotype. *Brain*. 2001;124(Pt 1):154-166.
26. Does MD, Beaulieu C, Allen PS, Snyder RE. Multi-component T1 relaxation and magnetisation transfer in peripheral nerve. *Magn Reson Imaging*. 1998;16(9):1033-1041.
27. Kollmer J, Kastel T, Jende JME, Bendszus M, Heiland S. Magnetization transfer ratio in peripheral nerve tissue: does it depend on age or location? *Invest Radiol*. 2018;53(7):397-402.
28. Wolff SD, Balaban RS. Magnetization transfer contrast (MTC) and tissue water proton relaxation in vivo. *Magn Reson Med*. 1989;10(1):135-144.
29. McGowan JC. The physical basis of magnetization transfer imaging. *Neurology*. 1999;53(5 Suppl. 3):S3-S7.
30. Dortch RD, Dethrage LM, Gore JC, Smith SA, Li J. Proximal nerve magnetization transfer MRI relates to disability in Charcot-Marie-Tooth diseases. *Neurology*. 2014;83(17):1545-1553.
31. Kollmer J, Hegenbart U, Kimmich C, et al. Magnetization transfer ratio quantifies polyneuropathy in hereditary transthyretin amyloidosis. *Ann Clin Transl Neurol*. 2020;7(5):799-807.
32. Kollmer J, Kessler T, Sam G, et al. Magnetization transfer ratio: a quantitative imaging biomarker for 5q spinal muscular atrophy. *Eur J Neurol*. 2021;28(1):331-340.

How to cite this article: Kollmer J, Weiler M, Sam G, et al. Quantitative magnetic resonance neurographic characterization of peripheral nerve involvement in manifest and pre-ataxic spinocerebellar ataxia type 3. *Eur J Neurol*. 2022;29:1782-1790. doi:[10.1111/ene.15305](https://doi.org/10.1111/ene.15305)